N91-10458

Optical and Morphological Properties of Cirrus Clouds Determined by the High Spectral Resolution Lidar During FIRE

Christian J. Grund and Edwin W. Eloranta
University of Wisconsin, Department of Meteorology
1225 W. Dayton St., Madison, WI. 53706

I. Introduction

Cirrus clouds reflect incoming solar radiation and trap outgoing terrestrial radiation; therefore, accurate estimation of the global energy balance depends upon knowledge of the optical and physical properties of these clouds. Scattering and absorption by cirrus clouds affect measurements made by many satellite-borne and ground-based remote sensors. Scattering of ambient light by the cloud, and thermal emissions from the cloud can increase measurement background noise. Multiple scattering processes can adversely affect the divergence of optical beams propagating through these clouds. Determination of the optical thickness and the vertical and horizontal extent of cirrus clouds is necessary to the evaluation of all of these effects. Lidar can be an effective tool for investigating these properties.

During the FIRE cirrus IFO in Oct.-Nov. 1986, the High Spectral Resolution Lidar (HSRL) was operated from a rooftop site (43^0 4' 29" N, 89^0 24' 26", 347.8 m msl) on the campus of the University of Wisconsin at Madison, Wisconsin. Approximately 124 hours of fall season data were acquired under a variety of cloud optical thickness conditions. Since the IFO, the HSRL data set has been expanded by more than 63.5 hours of additional data acquired during all seasons. This paper will present measurements of the range in optical thickness and backscatter phase function of cirrus clouds, as well as contour maps of extinction corrected backscatter cross sections indicating cloud morphology.

In our talk, we will present color enhanced images of range-time indicator (RTI) displays of a variety of cirrus clouds with ~30 sec time resolution. We will also demonstrate the importance of extinction correction on the interpretation of cloud height and structure from lidar observations of optically thick cirrus.

II. Technique

Because the lidar return signal from any range depends on both the backscatter cross section and the 2-way optical depth to that range, simple lidar systems, which make one measurement at each range, may not separately measure backscatter and extinction. Accurate knowledge of the extinction at one range, and a profile of the range dependence of the backscatter to extinction ratio (backscatter phase function), is essential to the determination of extinction from these lidar systems[1]. The HSRL differs from simple lidar systems in that it separates the particulate backscatter component from the molecular backscatter component of the lidar return.[2] Extinction is directly and unambiguously determined from the separated molecular backscatter return and an atmospheric density profile. This is possible because the atmospheric density determines the molecular backscatter cross section, thereby establishing a known target available at every range. The separation of molecular from particulate backscatter is achieved by observing differences in the spectral distribution of the scattered energy. The rapid thermal motion of the molecules Doppler-broadens the molecular backscatter spectrum. Particulates are more massive than molecules and are thus characterized by slower Brownian drift velocities which produce insignificant broadening of the scattered spectrum. The HSRL observes the return signal in two channels: a spectrally broad channel encompassing the molecular backscatter spectrum, and a spectrally narrow channel centered on the transmitted wavelength. With a system calibration[3], the 2-channel signals may be inverted to provide separate profiles of particulate and molecular scattering. Once the extinction is determined, the separated particulate scattering profile may be directly employed to determine the backscatter phase function.

III. Data Analysis

The particulate backscatter cross sections presented in fig.'s 1 - 4 were produced from inverted,

time averaged particulate and molecular scattering profiles acquired during fixed, vertically-pointing HSRL operations. They represent contour maps of the extinction corrected backscatter intensity of the cirrus clouds as they evolve in time and drift over the HSRL with the ambient winds. To reduce statistical noise, and mitigate the effects of aerosol-molecular channel cross talk, the HSRL in-cloud molecular backscatter signal has been obtained according to the following algorithm: 1) regions of small particulate-molecular channel cross talk (i.e. regions characterized by background aerosol and/or pure Rayleigh backscatter) are identified both above and below the cloud, 2) in these cloud-free regions, a least squares fit is produced of the observed molecular signal to the expected profile for a pure molecular scattering atmosphere calculated from a density profile, 3) the clear air observed signals are replaced with the smooth best fit estimates above and below the cloud, 4) the total cloud extinction is determined from the decrease in the best fit molecular signal across the cloud determined in step 3, while accounting for the expected decrease in molecular cross section with altitude, 5) on the assumption of a constant backscatter phase function and constrained by the optical thickness determined in step 4, a Bernoulli[4] solution for the extinction distribution within the cloud is produced from the inverted particulate backscatter profile, 6) the in-cloud molecular backscatter signal is replaced with a smooth estimate calculated from the extinction profile determined in step 5 and the known altitude distribution of of the molecular backscatter cross section. In this way, noise is removed from the molecular scattering profile, while the distribution of extinction is closely maintained.

Temporal averaging has been applied to the backscatter cross section profiles used to produce fig.'s 1 - 4. Noise considerations are such that 8-15 minute time resolution is possible at night, depending upon output power and upon cloud altitude and optical thickness. Daytime temporal resolution is somewhat degraded because of an increase in the background noise due to scattered sun light. Signal averaging times were chosen so as to limit the errors due to statistical fluctuations to ~ ±15% of the average in-cloud backscatter cross section for each profile. The resolution of the profiles used to produce fig. 1 is ~8 minutes and ~12 minutes for fig. 3. Fig. 2 has a time resolution ~1 hour, and the range resolution has been reduced to 900 meters in order to filter noise from the small particulate signals observed during that time period. Operations on Jan. 29-30, 1988 provided exceptional data, with 10 minute averaging possible during daylight and nighttime observations, even though the measured optical thicknesses occasionally exceeded 2.

The dashed lines presented in these plots represent a best estimate for an optical mid-cloud height. Half the cloud optical thickness is accumulated below this line as determined from the Bernoulli solution to the in-cloud extinction. Because the optical thickness of cirrus clouds may be generated by a highly irregular vertical distribution of extinction, this optical mid-cloud level could be useful in conjunction with (or instead of) cloud top and bottom altitudes in radiative transfer models.

IV. Discussion

On examining fig.'s 1-4 it is evident that cirrus clouds are produced in a variety of forms with large variations in cloud altitude and, thickness. For instance, during the ETO (10/30/87), we observed a ~100 m thick single layer cirrus cloud which persisted at 12.5 km for more than 1 hour. In contrast, fig. 4 (1/29-30/88) shows an 8 hour period of repeated, vertically developed cells, imbedded in an unbroken cirrus cloud layer having a vertical extent which occasionally exceeded 8 km.

Fig. 1 shows a contour plot of the backscatter cross section of an isolated cirrus cloud structure occurring on 10/27/86. Assuming no temporal development, and translation of the cloud with the ambient wind, the horizontal extent of this feature is estimated to be 48 km. The maximum value for the backscatter cross section was observed to be $4.4 \cdot 10^{-6}$ $m^{-1}sr^{-1}$.The average optical thickness of this cloud was .03 ±.006, with a bulk backscatter phase function of .028±.005 sr^{-1}.

Occasionally, background veils of optically thin (sub-visible) cirrus have been observed . Fig. 2 is a contour plot of such an event. In the vertical, this 3-5 km thick layer had an average optical thickness of .01±.004. It is important to note that the 19 m/s wind speeds at 10 km altitude imply a 266 km horizontal extent for this veil. One implication of such large scale "thin" cirrus is that remote sensors attempting to view horizontally within such layers could encounter optical thicknesses approaching 1 even though the cloud may not be visually apparent.

Fig. 3 depicts the backscatter cross section map of a cirrus cloud complex with a wind-drift-estimated horizontal extent of ~96 km. The maximum observed backscatter cross section was determined to be $2.4 \cdot 10^{-5}$ $m^{-1}sr^{-1}$. Profiles averaged between 5:40 and 7:40 GMT indicated a mean optical thickness of .58±.05 and a bulk backscatter phase function of .047±.007 sr^{-1}.

Fig. 4 shows an 8 hour segment of the backscatter cross section for a warm frontal cirrus system which occurred on 1/29-30/88. The maximum backscatter cross section of $4.3 \cdot 10^{-5}$ $m^{-1}sr^{-1}$ was observed near 1:30 GMT. Twenty minute averaged optical thickness varied between between .081 and 2.27 (see fig. 5), while the backscatter phase function varied from .031 - .057 sr^{-1} (see fig. 6). At the time of this writing, error bars had not been established for this data, but they should be comparable to previously reported values. It is interesting to note the large and systematic variation in backscatter phase function during a period of nearly constant optical thickness occurring between 18:00-20:00 GMT. This implies that a substantial portion of the structural information conveyed in fig. 4 is due to changes in the backscatter phase function and not just modulations of the extinction cross section. Thus, caution must be used in the application of simple lidar backscatter profiles to infer cloud radiative properties, even in a relative sense.

Table 1 summarizes the cirrus cloud optical thickness and bulk backscatter phase function estimates thus far completed. The mid-cloud optical altitude has been taken as representative for the determination of cloud temperature. These measurements represent only the analysed portion of the much larger HSRL cirrus cloud data set acquired since October,1986. They were produced from 15 - 120 minute data averages, and are indicative of the bulk properties across the entire cloud layer. The backscatter phase function dependence on mid-cloud temperature reported by Platt and Dilley[6] has not been observed in the HSRL data set.

V. Summary

Since the fall of 1986, we have observed cirrus clouds with backscatter cross sections ranging from $1 \cdot 10^{-7}$ - $4.2 \cdot 10^{-5}$ $m^{-1}sr^{-1}$, optical thicknesses from .001 - 2.3, and exhibiting backscatter phase functions in the range of .021 - .061 sr^{-1}. Persistent cirrus cloud layers have been observed with vertical thicknesses of ~.1 - 8 km. Coherent structural details ranging from 10's of meters and exceeding 250 km have been recorded. However, significant improvements in HSRL measurement statistics will be necessary to produce optical thickness and backscatter phase function measurements on time scales of less than 10 minutes, to reveal details of internal cloud optical properties, or to produce real time volume scans.

Fortunately, we are in the process of upgrading the system with a more powerful and spectrally stable laser which will decrease our time average requirements by a factor of ~40. This laser should also provide additional reductions in the aerosol-molecular channel cross talk terms, improving detailed analysis of backscatter phase function and extinction within cirrus clouds. It is possible that the HSRL will be operational with this new set of capabilities by the July 1988 meeting date.

This research has been supported under ARO grant DAAG29-84-K-0069 and ONR contract N00014-85-K-0581.

References

1. F. Fernald, B.M. Herman, J.A. Reagan, Determination of aerosol Height Distributions by Lidar, J.Appl.Meteor. **11**, 482, (1972).
2. C.J. Grund, Measurement of Cirrus Cloud Optical Properties by High Spectral Resolution Lidar, Ph.D. Thesis,
U.Wisconsin-Madison, (1987).
3. C.J. Grund and E.W. Eloranta, Interpretation of the Optical and Morphological Properties of Cirrus Clouds from Lidar Measurements, elsewhere in this volume.
4. J.A.Weinman, The Derivation of Atmospheric Extinction Profiles and Wind Speed Over the Ocean from a Satellite Borne Lidar, Submitted to App.Opt., (1988).
5. Platt, C.M.R. and A.C.Dilley, Determination of Cirrus Particle Single-Scattering Phase Function from Lidar and Solar Radiometric Data, App.Opt. **23**, 380, (1984).

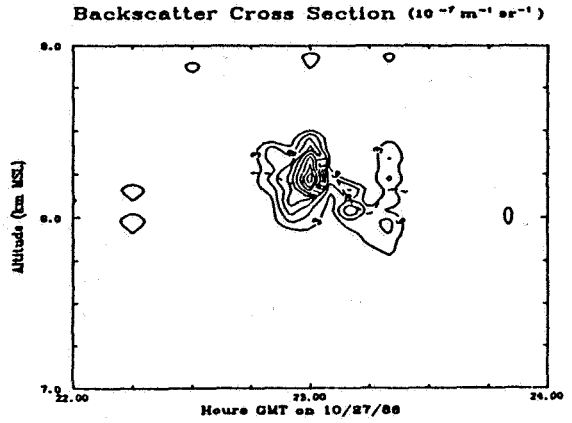

Fig. 1 Contour plot showing the particulate backscatter cross section (10^{-7} $m^{-1}sr^{-1}$) distribution within a cirrus cloud (___). The dashed line indicates the optical mid-cloud height (- - -, see text). The average optical thickness of this cloud was .03 with a bulk backscatter phase function of .028 sr^{-1}.

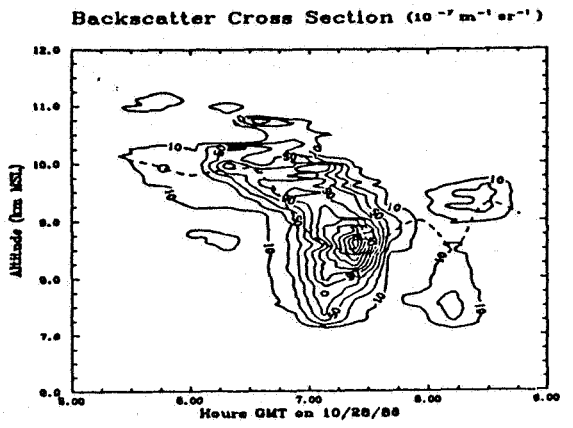

Fig. 3 Backscatter cross section (___) and mid-cloud optical height(- - -) of a cirrus cloud complex. Average optical thickness of this system was found to be .58 with a bulk backscatter phase function of .047 sr^{-1}. Contour units are 10^{-7} $m^{-1}sr^{-1}$.

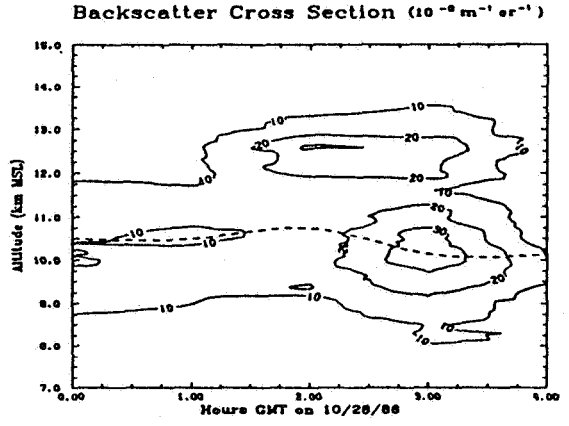

Fig. 2 Background veil of enhanced particulate backscatter may persist at cirrus cloud altitudes even when cirrus are not apparent. The range resolution has been reduced to 900 m to improve the noise statistics of this low backscatter data. Contour units are 10^{-8} $m^{-1}sr^{-1}$.

Table 1: Data Summary

Date	Time GMT	Altitude km	Optical Thickness	β_{π} sr^{-1}	T C^0	Δ Time Minutes
10/27/86	23.00	8.0	.03± 006	.028± 005	-32.6	20
10/28/86	6 00	9 8	.01±.004	.021±.009	-46 4	15
10/28/86	6 16	9.9	.09± 02	.023±.006	-47.1	15
10/28/86	6 31	10.0	.32±.095	.023± 006	-48.1	15
10/28/86	6 48	9 4	.38±.093	.032±.010	-42 5	15
10/28/86	7 03	8 4	.66±.18	.051±.016	-35 2	15
10/28/86	7:18	8 3	.85±.15	.054±.019	-34 3	15
10/28/86	7:34	8.6	.38±.11	.024± 008	-36.3	15
10/28/86	8:13	8 4	.21±.05	.023± 007	-35 2	15
10/28/86	8 29	9.2	.23±.08	.028±.007	-41.6	15
10/31/86	14:25	10 5	.11±.037	.030± 013	-59 0	45
10/31/86	15.05	10 2	.09± 034	.032± 016	-51.5	45
10/31/86	15.15	9.1	.12±.049	.024±.013	-41.5	45
10/31/86	16 25	8.8	.07± 032	.039±.018	-38.0	45
10/31/86	16 25	12.1	.02± 012	.023± 014	-66 5	45
10/31/86	17:05	8.8	.05±.019	.034±.015	-39.3	45
10/31/86	17:05	12.1	.01±.007	.045± 032	-66.5	45
7/24/86	7:24	10.2	.58±.07	.061± 008	-47.2	120
1/29/88	18 10	5 9	.62	.034	-28 6	20
1/29/88	18 30	6.8	.82	.035	-32.9	20
1/29/88	18 50	6.8	.86	.051	-33 9	20
1/29/88	19 10	5.8	.88	.059	-28.7	20
1/29/88	19 30	5.7	.74	.057	-27.8	20
1/29/88	19 50	6 9	.65	.034	-35 0	20
1/29/88	20 10	5 9	.83	.031	-28 9	20
1/29/88	20 30	6 8	.08	.035	-31 8	20
1/29/88	20 50	6 4	.40	.035	-31 8	20
1/29/88	21 10	7 8	.18	.039	-40 0	20
1/29/88	21 30	6.8	.90	.044	-33 9	20
1/29/88	21 50	6.8	.69	.048	-34 3	20
1/29/88	22 10	7.0	1.46	.052	-35 4	20
1/29/88	22 30	6 9	2.26	.052	-35 0	20
1/29/88	22 50	6 6	1.12	.048	-32 9	20
1/29/88	23 10	6.8	1 81	.041	-34 3	20
1/29/88	23 30	7 0	2.27	.038	-35 4	20
1/29/88	23 50	7.4	2 91	.043	-37 9	20
1/30/88	0 10	6 9	.74	.052	-35 0	20
1/30/88	0 30	7 1	1 84	.041	-35.7	20
1/30/88	0 50	9 2	1.03	.035	-48 7	20
1/30/88	1.10	7.9	1.46	.049	-40 8	20
1/30/88	1:30	7 5	.93	.045	-38 6	20
1/30/88	1:50	9.9	.67	.030	-52 7	12

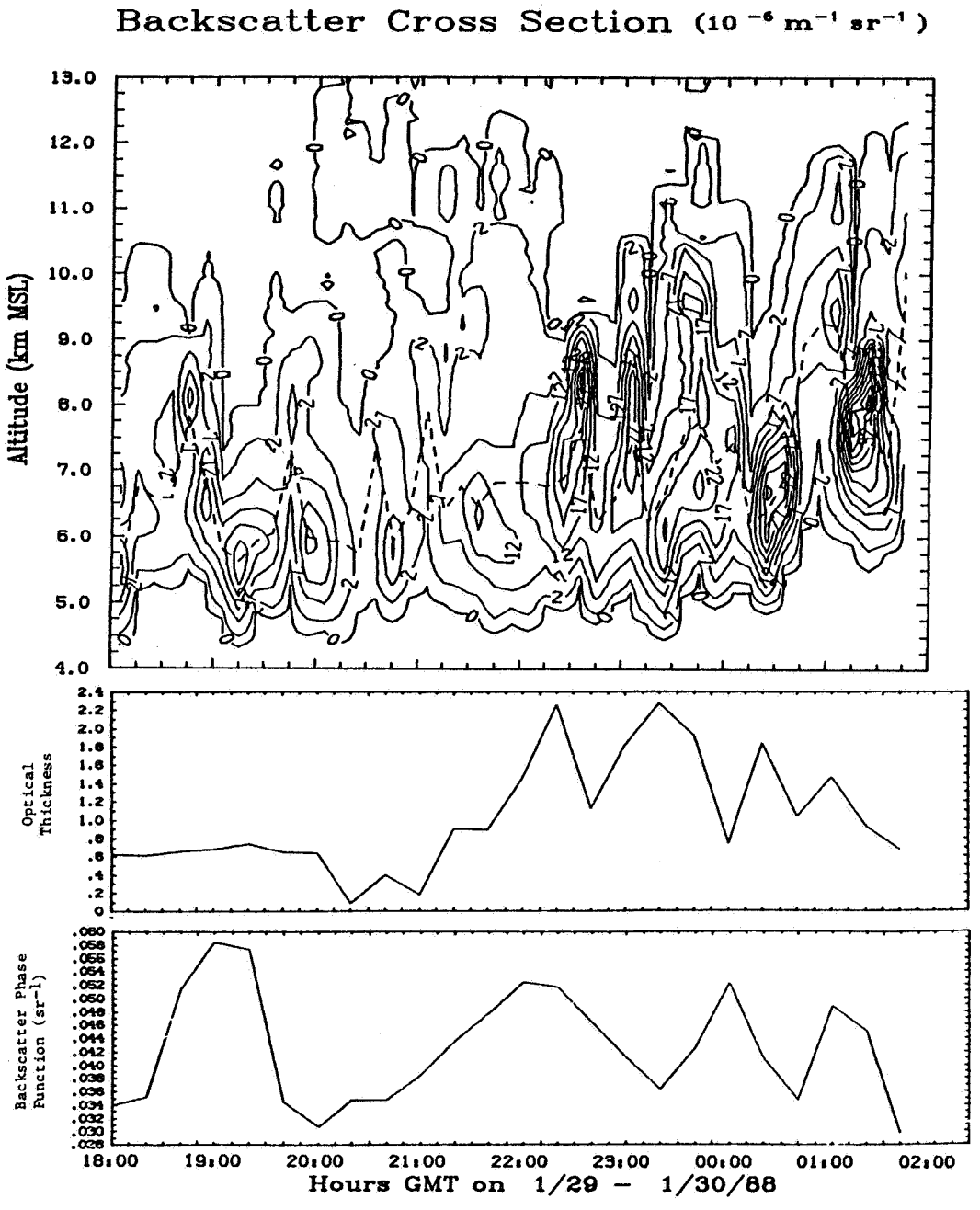

Fig. 4 (top) Backscatter cross section (——) and mid-cloud optical height (- - -) of a cirrus cloud shield preceding a warm front. Notice the series of repeated cells of enhanced backscatter. Modulations of the mid-cloud height (1-2 km) are closely tied to the cell patterns. **Fig. 5** (middle) Optical thickness record for 1/29-30/88 (20 minute independent averages). **Fig. 6** (bottom) Backscatter phase function record for 1/29-30/88 (20 minute independent averages). Note the large systematic change in the backscatter phase function during the first 2 hours of the data set. This change occurred even though the average optical thickness remained constant, indicating that much of the structural information conveyed in fig. 4 was not simply produced by modulation of the extinction. Thus, caution must be used in the application of simple lidar backscatter profiles to infer cloud radiative properties, even in a relative sense.